Journal of Vibration and Acoustics 126(1) 118-125.

IDENTIFYING COULOMB AND VISCOUS FRICTION IN FORCED DUAL-DAMPED OSCILLATORS

First author: Jin-Wei Liang,
Institute: Department of Mechanical Engineering, MingChi Institute of Technology,
Address: 84 Gung-Juan Rd., Taishan, Taipei County, Taiwan, 24306, Republic of China.
Telephone: 886-2-29089899 ext. 4247
Fax: 886-2-29041914
email: liangj@ccsun.mit.edu.tw

Second author: Brian F. Feeny,
Institute: Department of Mechanical Engineering, Michigan State University,
Address: 2328C, Engineering Bldg., East Lansing, MI 48824, USA.
Telephone: (517) 353-9451
Fax: (517) 353-1750
email: feeny@egr.msu.edu

ABSTRACT

This paper presents a method for estimating Coulomb and viscous friction coefficients from responses of a harmonically excited dual-damped oscillator with linear stiffness. The identification method is based on existing analytical solutions of non-sticking responses excited near resonance. The method is applicable if the damping ratio of viscous component can be considered small. The Coulomb and viscous friction parameters can be extracted from two or more input-output amplitude pairs at resonance. The method is tested numerically and experimentally. Experimental results are cross checked with estimations from free-vibration decrements and also from friction measurements.

1 INTRODUCTION

In this paper, we present a method of simultaneously estimating Coulomb and viscous damping parameters in forced linear oscillators. The method complements existing vibration-based methods for identifying single-source and dual-source damping in free and forced vibration, and rivals such methods in simplicity. In this work, we apply the method to a linear-bearing experiment, for which Coulomb plus viscous friction serves as a simplified model.

Mechanical vibration systems with viscous and Coulomb friction are of importance in the applications of dynamics and control problems. Den Hartog [1] first solved the forced response of a single-degree-of-freedom system with both viscous and dry-friction damping. His results included the analytical solutions of periodic non-stop and stick-slip motions, and illustrations of the frequency response curves for different values of viscous damping, dry-friction damping, excitation amplitude, and excitation frequency. Hundal [2] studied a base-excitation frictional oscillator in which close form analytical solutions of the equation of motion were obtained. Results were presented in nondimensional form as magnification factors versus frequency ratios as functions of viscous and Coulomb friction parameters.

Various approaches have been adopted to identify damping information from a vibration system with both sources of damping. For example, Jacobsen and Ayre [3] developed an approximate scheme for estimating both viscous and dry friction quantities from the free-vibration decrements by noting that the viscous friction dominates in the large-amplitude responses, and that Coulomb friction dominates in the small-amplitude oscillations. As such, they exploited the exponential and

linear decay of a free vibration viscous or Coulomb-friction damped system, knowledge of which goes back to Helmholtz [4] in 1863 and Rayleigh [5] for the viscous case, and Lorenz [6] for the Coulomb case. Watari [7] presented an exact scheme for extracting viscous and dry friction estimates. We recently derived an equivalent scheme and applied to a controlled experiment [9] and also an industrial linear-bearing system [8].

The methods above, however, rely on sufficient excursion magnitudes of the free-vibration response. If enough damping is present, such responses may not be possible. To this end, it makes sense to develop methods for identifying friction parameters in forced oscillators. Tomlinson and Hibbert [10] used the power dissipation to estimate Coulomb and hysteretic damping coefficients. Tomlinson [11] also used the distortions in the complex receptance plots to estimate damping parameters, and Chen and Tomlinson [D] proposed estimating damping parameters in nonlinear oscillators by using the displacement, velocity and acceleration output and formulating the output in terms of series of frequency response functions. Iourtchenko et al. [A], based on Dimentberg [B], applied a harmonic balance analysis to generate identification equations. Iourtchenko and Dimentberg [C] used stochastic averaging to identify nonlinear damping in-process when the excitation was random. Stanway et. Al. [12] proposed a nonlinear least-squares estimator scheme which involves the on-line solution of several additional equations. Yao et al. [13] obtained the Coulomb and viscous friction parameters by using a recursive nonlinear least-squares algorithm.

This work employs the findings of Den Hartog [1] and Hundal [2] for the nonsticking response to harmonic excitation at resonance, and results in a simple algorithm for identifying viscous and dry-friction damping from mechanical vibration systems. Both viscous and Coulomb friction are assumed to coexist. The method uses an assumption that the viscous damping ratio is small enough that the frequency of damped oscillation is approximately equal to the undamped natural frequency. Numerical simulations of a model of an industrial linear-bearing system are conducted to estimate both the viscous and dry-friction damping existing in the system. Experimental results are presented, verified and discussed. The dynamic friction characteristics of the linear-bearing system are also examined.

2 FORCED RESPONSE AND FRICTION IDENTIFICATION

A mass-spring-damper system on a rigid surface with the Coulomb friction law can have either stable pure-sliding or stick-slip motion when subjected to harmonic base excitations (Hundal [2], Shaw [16], Marui and Kato [17]). We consider a mechanical vibration system with an external viscous damper and dry-friction contact as a model of an industrial linear-bearing system with both viscous and dry friction chosen to represent the damping in the ball bearings and the linear guide. A schematic diagram depicting the linear single-degree-of-freedom oscillator with viscous and Coulomb friction and base excitation is presented in Figure 1. Our model is different from that presented in Hundal's report [2], namely instead of placing the viscous element in parallel with the spring (i.e. between the moving base and the mass), we put both the viscous and Coulomb elements between the mass and ground. The system is configured in accordance with the mechanical structure of the linear-bearing system. The model of the system shown in Figure 1 consists of a second-order differential equation which is piecewise linear and solvable. The equation of motion can be written as

$$m\ddot{x} + c\dot{x} + kx + F(\dot{x}) = ky(t), \tag{1}$$

where $m, c,$ and k are the mass, damping coefficient, and spring constant, $y(t) = Y_o \cos(\omega t + \phi)$ is the base excitation motion and $F(\dot{x}) = F_o \operatorname{sgn}(\dot{x})$ is the Coulomb friction force. Definition of the friction force for $\dot{x} = 0$ is not necessary since sticking motion is not to be considered in this work.

The governing differential equation shown above is essentially the same as that in Den Hartog [1]. For the case of $\dot{x} < 0$,

$$\ddot{x} + \frac{c}{m}\dot{x} + \omega_n^2 (x - x_f) = \omega_n^2 Y_o \cos(\omega t + \phi), \tag{2}$$

where $x_f = F_o / k$ denotes the equivalent "friction displacement". Den Hartog [1] showed that in certain parameter regimes, there exist nonsticking responses with peak values x_o, which occur at the turning points. The value of x_o is governed by

$$\frac{x_o}{Y_o} = -G\left(\frac{x_f}{Y_o}\right) + \sqrt{\frac{1}{q^2} - H^2\left(\frac{x_f}{Y_o}\right)^2} \tag{3}$$

where G and H are parameter functions independent of the Coulomb friction, and can be represented as

$$G = \frac{\sinh(\zeta\beta\pi) - \zeta / \sqrt{1-\zeta^2}\sin(\omega_d \pi / \omega)}{\cosh(\zeta\beta\pi) + \cos(\omega_d \pi / \omega)} \tag{4}$$

$$H = \frac{\beta / \sqrt{1-\zeta^2}\sin(\omega_d \pi / \omega)}{\cosh(\zeta\beta\pi) + \cos(\omega_d \pi / \omega)}, \tag{5}$$

where q is the inverse response function with pure viscous damping:

$$q = \sqrt{\left[1 - \left(\frac{\omega}{\omega_n}\right)^2\right] + \left(2\zeta\frac{\omega}{\omega_n}\right)^2} \tag{6}$$

In the above expressions, ζ is the nondimensional damping ratio, $\beta = \omega_n / \omega$, and $\omega_d = \omega_n\sqrt{1-\zeta^2}$ represents the frequency of damped oscillation.

Note that G and H in Eqs. (4) and (5) are functions of ζ, ω_n, and ω only. Given a system with fixed parameter values, these parameter functions can be treated as constants in the derivation of the estimate algorithm.

As such, we propose an identification approach based on the analytical input-output expression (3). We assume that ζ is small, which is reasonable for the linear-bearing system to be investigated [18]. Meanwhile, from Eq. (5), $H = 0$ when $\omega = \omega_d$ and $\zeta \neq 0$. Experimentally, if we excite a low viscous-damping system near its resonance such that $\omega = \omega_n \approx \omega_d$, we can assume $H \approx 0$ (when $\zeta \neq 0$). (In fact, as $\zeta \to 0$ and $\omega \to \omega_n$, $H \to 1/\pi$, which is small compared to $1/q \to \infty$ in Eq. (3).) Neglecting H at resonance, the input-output amplitude relationship in Eq. (3) reduces approximately to

$$x_o = -Gx_f + \frac{Y_o}{q}. \tag{9}$$

Hence, x_o and Y_o approximately satisfy a *linear* relationship, from which the slope and intercept define q and $x_f G$ (and thus ζ and x_f).

Under conditions corresponding to two excitation levels with the same frequency (close to the damped natural frequency) with input output pairs denoted as (Y_1, x_1) and (Y_2, x_2), we have

$$x_1 = -Gx_f + \frac{Y_1}{q}, \tag{10}$$

$$x_2 = -Gx_f + \frac{Y_2}{q}. \tag{11}$$

whence

$$q = \frac{Y_2 - Y_1}{x_2 - x_1}, \tag{12}$$

and

$$x_f = \frac{x_1 Y_2 - x_2 Y_1}{G(Y_1 - Y_2)}. \tag{13}$$

If $\omega \approx \omega_n \approx \omega_d$, then, using Eq. (6), Eq. (12) is approximated in terms of ζ as

$$\zeta \approx \frac{Y_2 - Y_1}{2(x_2 - x_1)}. \tag{14}$$

Also, G reduces in approximation to

$$G \approx \frac{\sinh \zeta\pi}{\cosh \zeta\pi - 1}. \tag{15}$$

It makes sense to use this approximation if the assumption $\omega_d \approx \omega_n$ is employed, without clear distinction of whether $\omega = \omega_n$ or $\omega = \omega_d$ in the experimental test. If more than two input-output amplitude pairs are measured, the intercept and slope of Eq. (9) can be estimated by a least-squares fit of the (Y_i, x_i) data.

While the proposed method is based on the analytical results of Den Hartog's work, the identification algorithm is very simple and easy to be implemented provided that the target system behaves closely to the Coulomb plus viscous model. In implementing the identification process, the system is required to be excited at the resonance. Such an excitation frequency requirement is also needed in the methods proposed by Tomlinson for more accurate estimations [10-11]. In the next section, we present numerical verifications and a variational study, focusing on the amplitude perturbations. These numerical studies will be followed by experiments with a linear-bearing system.

3 NUMERICAL INVESTIGATIONS AND ERROR ANALYSIS

In this section, we investigate the forced-resonance algorithm numerically. First, we apply the input-output amplitude relationships listed in Table 1 to the forced-resonance algorithm presented in Eqs. (13)-(14). The input-output relationships shown in Table 1 were obtained using the analytical relationship (3), while numerical integrations with respect to the system governing differential equation (Eq. (1)) were conducted occasionally to assure the occurrences of the pure-sliding motion. Numerical values of system parameters corresponding to Eq. (1) are $m = 1.0, k = 100.0, c = 4.0, F_o = 2.0, \omega = 10.0$. The estimated results as well as the accuracies are

listed in Table 2. Note that to implement the estimating process, we substituted (Y_1, x_1) and (Y_4, x_4), rather than (Y_2, x_2), into Eqs. (13) and (14). Meanwhile, for calculating "G", the exact expression (4) was adopted instead of the simplified expression (15). The estimated results changed very little if the simplified expression (15) was used. With the chosen value of ζ, there is no big difference between the damped and undamped natural frequencies, and the assumptions needed for applying the method are valid. It can be seen in Table 2 that the estimation results are very close to the known parameter values, which shows the reliability of the identification algorithms.

Next, we would like to understand how amplitude measurement perturbations could affect the accuracy of estimation. To that end, we start with a variational study of the input and output amplitudes to obtain, to first order, the error induced in the identification equations. For the variational study, we conduct Taylor expansions with respect to Eqs. (13) and (14). Keeping first order terms, we have

$$\delta\zeta = \frac{1}{2(x_2 - x_1)}\left\{\delta Y_2 - \delta Y_1 - 2\zeta(\delta x_2 - \delta x_1)\right\} \tag{16}$$

and

$$\delta x_f = A\delta x_1 + B\delta x_2 + C\delta Y_1 + D\delta Y_2 + E\delta\zeta \tag{17}$$

in which

$$A = \frac{Y_2}{G(Y_1 - Y_2)}$$

$$B = \frac{-Y_1}{G(Y_1 - Y_2)}$$

$$C = \frac{Y_2(x_2 - x_1)}{G(Y_1 - Y_2)^2}$$

$$D = \frac{Y_1(x_1 - x_2)}{G(Y_1 - Y_2)^2}$$

$$E = \frac{(x_2 Y_1 - x_1 Y_2)}{G^2(Y_1 - Y_2)}\frac{\partial G}{\partial \zeta}$$

From Equations (16) and (17), we realize that to minimize the variation of ζ, i.e. $\delta\zeta$, we should maximize the difference of response amplitudes, $(x_2 - x_1)$. Also, $\delta\zeta$ depends weakly on the output error if ζ is small. Moreover, careful inspection of the expressions of δx_f, A, B, C, D, and E indicates that to minimize δx_f, we need to maximize difference between input amplitudes, $(Y_1 - Y_2)$, which again will minimize $\delta\zeta$. This makes sense, since we are approximating the slope and intercept of a straight line. Therefore, to increase the estimation accuracy in this forced-identification method, we would want to take two input-output amplitude pairs as separated as possible. Furthermore, the quantities A through E decrease with decreasing ζ, through the value

of G, and hence we expect smaller errors in the Coulomb parameter if ζ is small

Anytime there is error in the measurement, there will be error in the estimated parameters. While not presented here, we studied numerical examples to gain some insight into how measurement errors affect the identification results. In an example, a 5% of single amplitude-measurement in Y_1 led to a 22.64% error of the Coulomb-parameter estimation, F_o. The sensitivity of the Coulomb parameter to the measurement error can be found in other schemes [8]. This happens here because the Coulomb parameter estimation is dependent on the estimation of ζ. In the next section, we will apply this estimation method to a linear bearing experiment.

4 EXPERIMENTAL ESTIMATIONS

Figure 2 shows a photograph of the experimental set-up investigated in this study. The experimental system consists of two linear-bearing systems (THK SR20UU with four linear motion (LM) blocks), an electromagnetic shaker with a power amplifier (B&K 4809 and 2706), two LVDTs with signal conditioners (Rabinson-Halpern Co., Model 210A-0500), an accelerometer with a charge-type amplifier (B&K 4371 and 2635), and a data-acquisition system including software and hardware (LabVIEW and NI-AT-MIO-16E-10). The LVDTs were used to sense the displacement responses and the accelerometer was adopted to check if the responses are close to pure sliding motions. The resolution of LDVT after the quantization step in data-acquisition process is about 3 μ m.

Mechanical parameters of this system are $m = 1.042$ kg, $k = 1568$ N/m, $\omega_n = 6.2$ Hz. Here, the stiffness of the helical springs was determined by a free-vibration test. Knowing the value of the sliding mass, the stiffness can be calculated based on the system's natural frequency while neglecting the viscous damping effect. We consider a Coulomb plus viscous oscillator with "low damping" for small ζ in this paper. Our previous work with helical springs [8] suggests to us that the "low damping" in the bearing is much larger than what would be in the spring. To this end, the damping in the helical spring will be neglected in this study.

The linear-bearing systems are unique motion systems in which linear motion is supported by rolling contact elements. Linear-bearing systems have been widely employed as components of machine tools, machining centers, industrial robots, semi-conductor production equipment, medical equipment, and many other electronically controlled devices. To design a satisfactory controller that accounts for the effects of the intrinsic resistance, complete understanding of the friction dynamics of the system is necessary. Existing reports on the investigations of dynamic features of the linear-bearing systems include references [19-21]. These, however, focus primarily on the design procedures and concepts of the linear-bearing systems.

In conducting our experimental investigations, harmonic signals were applied to drive the electromagnetic shaker so as to acquire nonsticking responses of the sliding table. Nearly pure-sliding motions were achieved. Such pure sliding motions were nearly sinusoidal except for some distortions occurring at direction reversals [16].

Next, the excitation levels were varied while the frequency was held fixed at resonance. Thus, the $H \approx 0$ assumption made in the forced-resonance method was fundamentally satisfied. Five sets of input-output amplitude responses were obtained. Every input (or output) time-domain history, which lasted more than ten forcing cycles, was applied to an averaging process to gain one input (or output) amplitude measurement. Finally these input-output amplitude pairs were recorded. In order to gain more confidence in the method, we conducted many more experiments near the system's resonance. The experimental input-output amplitude relationships are plotted in Figure 3. In this figure, every small square represents one pair of input-output amplitudes. Each pair of input-output amplitudes was obtained by averaging time-domain histories sustaining more than ten forcing cycles.

When conducting the experiments, we increased the excitation levels stepwise to obtain various

input-output amplitude responses. We repeated this sweep several times and data were plotted in the chronological order of the experimental process. Therefore, each slanted line in Figure 3 depicts an amplitude sweep. There are five excitation levels in each amplitude sweep, and totally, ten similar amplitude sweeps are contained in Figure 3. Connecting the data with lines in a chronological plot in Figure 3 brings forth interesting information. Since the lines are nearly parallel, the slope does not change much in time, and hence ζ does not change much in time. Since the lines are not coincident, they are shifting up and down in time, such that the intercept changes in time, meaning the Coulomb friction parameter changes in time. The Coulomb friction parameter seems to vary more than the viscous friction parameter. However, the variation in the Coulomb parameter occurs on a slow enough time scale that the lines remain nearly parallel.

In the same figure, the bold slanted line is the least-squares linear fit of the input-output data. Based on Eq. (9), the slope of this bold line is closely related to the averaged estimation of ζ, whence we obtained $\widetilde{\zeta}_1 = 0.0987$. The ζ estimation is then applied to obtain the parameter G ($G = 6.44$ calculated from Eq. (4)) which in turn is applied to obtain the intercept of Eq. (9) for the x_f estimation. We obtained an averaged estimation of $\widetilde{x}_{f1} = 2.80$ mm. This value can be converted into an averaged friction force $\widetilde{F}_{o1} = 4.39$ N. The producer of the linear-bearing systems has provided a conservative gross value of the *maximum* end-seal resistance, which is equal to 3.4 N for the product we picked [18]. This value is referred to a single LM block, but we have four LM blocks in our experimental set-up. Therefore, the *maximum* friction force could be as large as 13.6 N based on the manufacturer's data. Thus, the estimated value is in the reasonable range. The maximum friction force depends greatly on whether the bearing seals are mounted. In this study, the friction force can be attributed mainly to the resisting force exerting by the end seals [18]. Meanwhile, people might be puzzled by the seeming high friction force (4.39 N) seen in this study in comparison with the loading (about 10 N). These two values give the coefficient of friction to as high as 0.439. The value is reasonable because of the extremely light loading case that corresponds to unbounded and unspecified coefficients of friction based on the manufacturer data [18] (i.e. the bearings are resistive even when unloaded).

According to the theory, we expect the data in Figure 3 to fall on a straight line. But we see a distortion in the curve, mostly at higher amplitudes. The lower-amplitude portion of the x, Y plot shown in Figure 3 indicates that for a rather robust range of input/output amplitudes, the slope and intercept do not change much. For the larger amplitude response, the deviation from the linear x, Y plot is more concentrated. The deviation from the straight line at higher amplitudes may arise from the small ζ assumption, or possibly from other sources of nonlinearity, such as unmodeled dynamic friction effects, or stiffening springs. In order to clarify whether the deviated part of the data is caused by the simplification of Eq. (3) via a small ζ assumption, we did a simulation of the x, Y plot for a nonlinear analytical input/output relationship with parameter values as identified in this experiment. The analytical curve is presented as a bolded-dotted line in Figure 3. It can be seen in Figure 3 that the simulated x, Y analytical curve is visually indistinguishable from the straight line obtained from the least-squares criterion. Hence the deviation from linearity is not due to small-ζ approximation in the identification scheme, used in both the simulation and the experiment, rather it is due to modeling error. Furthermore, simulations with a stiffening spring did not generate a deviation from a linear *x, Y* plot. However, since the deviation from x, Y linearity is more concentrated for larger amplitude of x and Y, it is possible that the system behavior deviates more from the model behavior in that range.

To this end, for the sake of comparison, we estimated the parameters from the lower 4/5, 3/5, and 2/5 of the data, taken to be portions of the data that are on progressively straighter portions of the data set. The estimates corresponding to these data subsets were $\widetilde{\zeta}_{4/5} = 0.114$ and $\widetilde{x}_{f_{4/5}} = 2.63$ mm ($\widetilde{F}_{o_{4/5}} = 4.12$ N), $\widetilde{\zeta}_{3/5} = 0.126$ and $\widetilde{x}_{f_{3/5}} = 2.49$ mm ($\widetilde{F}_{o_{3/5}} = 3.91$ N), and $\widetilde{\zeta}_{2/5} = 0.142$ and

$\widetilde{x}_{f_{2/5}} = 2.35$ mm ($\widetilde{F}_{o_{2/5}} = 3.69$ N), respectively.

In the next section, we perform additional experiments using the free-vibration decrement method and the indirect measurement of the dynamic friction behavior. The results are used to verify the ζ and x_f estimations made by the forced-resonance identification approach.

5 VERIFICATION OF THE EXPERIMENTAL ESTIMATIONS

5.1 Free Vibration Decrements

A primary motivation for developing a forced-vibration identification approach as an alternative to the free-vibration approach is that some systems have parameter values which do not produce sufficient oscillatory excursions needed for the free-vibration method. To validate the experimental damping estimations made in the last section, we first applied the free-vibration decrement method [8,9] to the same linear-bearing system. However, the experimental parameters used in Section 4 were not suitable for the free-vibration test since the helical springs were too soft to provide enough free oscillation excursions for the estimating process. (This is the case even though the viscous damping component is deemed "small".) So we replaced the helical springs with a stronger set, which had a stiffness of 4365 N/m rather than 1568 N/m. According to the motivation, we chose to retain the softer springs in the forced-vibration study and then switch to the stiffer springs to enable a crosscheck based on the free-decrement approach. Based on the assumption that the damping in the bearing dominates the damping in the springs, we assume that the system damping coefficients change little due to the change of system stiffness. It it possible, however, for unmodeled dynamic friction behavior to vary somewhat with the oscillation frequency, which changes with the new springs. Nonetheless, we conducted a set of free-vibration tests with stiffer springs in order to estimate the damping information from the system.

Each free-vibration test sustained about two periods of oscillation. Therefore, from the extreme excursions, five amplitude measurements were recorded in each test. These five free-vibration amplitudes provided two sets of viscous and dry-friction estimates in accordance with the decrement method [8,9]. We present the results in Table 3. In Table 3, the first two columns of data, representing one set of damping estimations, were obtained from the first four amplitudes in each free-vibration test, whereas the last four amplitudes in the same test generated the last two columns of data.

We calculated the average value of estimations addressed in Table 3. First the averaged $\widetilde{\zeta}$, denoted as $\widetilde{\zeta}_2$, is equal to 0.0819, which is the mean value of 34 estimations. Similarly, the averaged x_f, is $\widetilde{x}_{f2} = 0.807$ mm. $\widetilde{F}_{o2} = k\widetilde{x}_{f2} = 3.52$ N. Since $\zeta = c/2\sqrt{mk}$ and $x_f = F_o/k$ depend on the stiffness, which was changed in order to perform the decrement method, these numbers need adjustments in order to be compared with the estimates obtained using the forced-resonance method. As such, the viscous damping factor and Coulomb-friction distance estimates, in terms of the soft-spring system, are $\widetilde{\zeta}_{2eq} = 0.0819 \times \sqrt{4365/1568} = 0.137$ and $\widetilde{x}_{f2eq} = 0.807 \times 4365/1568 = 2.25$ mm. Thus, good agreements exist between the viscous estimates obtained from the free-vibration decrement method, $\widetilde{\zeta}_{2eq}$, and the corresponding results obtained from the forced-resonance method with either the lower 3/5 or 2/5 part of data (where the input-output data deviated little from the straight-line model), namely $\widetilde{\zeta}_{3/5}$ and $\widetilde{\zeta}_{2/5}$ in the previous section. Similar consistencies also exist among corresponding Coulomb-friction estimates using both free- and forced-vibration identification schemes.

Table 4 summarizes the average experimental estimations obtained by the forced-resonance identification algorithm and the free-vibration algorithm together.

5.2 Dynamical Friction Behavior

In interpreting our results, it may be worthwhile to understand the friction behavior in the system. Although the identification model consists of Coulomb and viscous friction, the true friction dynamics existing at the interfaces of the linear-bearing system is completely unknown. In order to characterize the friction, it must first be measured. To do this, we calculated the friction force from the system's ODE together with motion measurements [22]. Alternatively, we could measure the friction with a load cell, but since the friction element is somewhat bulky linear bearing, we opted for the former method. The indirect friction-measurement method, while requiring several motion signals to be manipulated in accordance with the equation of motion, has provided consistent friction measurement as compared to the direct method in other frictional vibrating systems [22,23].

Generalizing Eq. (1), we consider the unknown friction $F(x,\dot{x})$ to depend on both the relative displacement and velocity at the contact interfaces. The experimental parameters are $m = 1.042$ kg, $k = 1568$ N/m, and $\zeta \approx 0.0987$. Additionally, calculation of the friction force from Eq. (1) required the measurement of all of the motion signals: input and output displacements, $\tilde{y}(t)$, $\tilde{x}(t)$, the velocity response, $\tilde{\dot{x}}(t)$, and the acceleration response $\tilde{\ddot{x}}(t)$. In this regard, two LVDTs were used to sense the input and output displacement responses, whereas an acelerometer was used to measure the acceleration. The velocity signal was obtained by differentiating the displacement signal, and was then smoothened with a five-point moving average. By looking at harmonic responses of a mass-spring system in an air track, and ensuring that the displacement and acceleration were 180 degrees out of phase, we corrected the phases of sensor signals.

Figure 4 illustrates a typical time-domain history that contains all the motion responses and the extracted friction force. Figure 5 depicts the relationship between the calculated friction force and the relative velocity. In the friction force presented in Figures 4 and 5, an averaged viscous-damping component with $\zeta = 0.0987$ has been applied and removed from the friction data.

The motion exhibited in Figure 4 is close to a pure sliding motion. This can be justified by examining the velocity or acceleration signals [24]. Furthermore, there are many dynamic friction features addressed in Figures 4 and 5. For example, there are slanted transitions in force-velocity characteristics in the vicinity of zero velocity in Figure 5. The occurrence of this slanted hysteretic feature can be caused by contact compliance [25, 26]. Contact compliance may arise from elastic deformation near the contact point, which in this system could mean the contact between end seal and linear guide, internal components, or in the surrounding structures.

Moreover, though it is not included here, the contact compliance can be estimated from a friction-displacement plot or from an impulse test at a sticking condition [24,25]. We have estimated the value of the contact stiffness of this system with both methods. The approximate contact stiffness is 11.6×10^4 N/m. This value can be placed in the following equation for estimating the transition velocity corresponding to the onset of macroscopic sliding motion [24,25]

$$V_s = 2\omega\sqrt{\frac{X_m F_k}{K_y} - \left(\frac{F_k}{K_y}\right)^2} \tag{18}$$

where ω represents the excitation frequency, F_k is the kinetic friction component, X_m is the maximum displacement of the sliding mass, and K_y denotes the contact stiffness. If we take $K_y = 11.6\times10^4$ N/m, $X_m = 4.25\times10^{-3}$ m, $\omega = 38.5$ rad/s estimated from Figure 4***Check number), $F_k = 3.5$ N (estimated from Figure 5), the estimation of transition velocity turns out to be 0.028 m/s, which corresponds well to the transition velocity shown in Figure 5 (about 0.024 m/s).

Agreement of the transition velocity supports the contact compliance model. Dynamical friction associated with contact compliance is not rare to observe; other recent reports include, e.g. Hinrichs, Oestreich, and Popp [26], Harnoy et al. [27], McMillan [28], and Feeny and Kappagantu [29].

There are other friction dynamics presented in Figures 4 and 5. For instance, stochastic force fluctuations can be observed during the sliding phase in both figures. Many researchers [25,27,32] have reported similar stochastic sliding friction. An additional memory effect emerges in Figure 5 manifesting itself by the difference of friction magnitudes at accelerating and decelerating portions of motion. The friction magnitude decreases immediately prior to the slip-to-stick transition. This feature suggests that the friction force hysteresis depends not only on the contact compliance, but also on the history of sliding.

The feature is obvious in the stick-slip case. In Figure 6, the force reaches its peak in the stick-to-slip transition, so the small hysteresis loops are clockwise. The hysteresis due to contact compliance can appear as small loops in the vicinity of zero velocity in the *f-v* plots of stick-slip responses [25,26]. Thus, the hysteresis remaining is due to other effect.

Since we accounted for the viscous friction component by using the identified value of ζ ($\widetilde{\zeta}_1 = 0.0987$) in the force computation, we would expect the force to be flat, on the average, during the sliding interval. Nevertheless, the slope of the data in Figure 3 indicates a larger effective viscous term for low-amplitude responses than for high-amplitude responses. (***I deleted this because I don't understand it***) Our higher amplitude responses are consistent with that of Figure 5 regarding the average force level and the contact compliance behavior. Overall, the Coulomb and viscous friction are consistent with the estimated friction histories. Since the friction behavior seems to include small dynamical effects not included in the straight Coulomb and viscous model, it is reasonable to have some deviation. Indeed, contact compliance and other effects can have an effect on the input-output dynamical behavior of the oscillator [30,32-37], and so the response amplitudes of the compliant system will differ slightly from those of rigid-contact system, even if the contact is quite stiff. To adequately address friction dynamics observed in the linear-bearing system, friction models other than Coulomb plus viscous can include, for instance, the models of Soom and co-workers [38], the state variable models of Rice [39], Deterich [40], and Ruina [41], the bristle models of Canudas de Wit *et al.* [42] and Haessig and Friedland [43], the normal vibration models of Oden and Martins [44], Tolstoi [45] and Dankowicwz [46], and the contact compliance models [25-27]. Ultimately, we have to choose a model before we estimate model parameters. We feel that the Coulomb plus viscous is a very worthy model to use as a starting point, as its simplicity makes dynamical analyses tractable. As such, this work is that of damping-parameter identification, rather than friction-law identification.

6 CONCLUSIONS

In this paper, a friction-parameter identification algorithm was proposed. The identification method is suitable for harmonic excitations of a single-degree-of-freedom system with Coulomb and viscous friction and linear stiffness. To apply the method, the excitation must occur at resonance, and the contribution of the viscous damping must be low enough such that $\omega_d \approx \omega_n$. The resulting identification equations represent a linear relationship between the input and output amplitudes, from which the slope and intercept lead to estimates of the Coulomb and viscous friction parameters.

Numerical simulations of the method with respect to an unperturbed system illustrated excellent accuracies in damping estimations. In the presence of noise, widely spaced input-output data lead to the best results for two-point estimations.

We applied this new forced-identification algorithm to a linear-bearing system. The damping estimations obtained by this method were repeatable. Furthermore, in the same linear-bearing

system, results estimated by the forced-resonance method were consistent with those obtained by both a free vibration method and by indirect friction force measurements, even though the latter revealed the presence of subtle dynamical friction behavior. We found that although the viscous damping factor was considered "small" enough for the resonance method, the total damping was large enough that the free-vibration method could not be applied without modification of the system stiffness.

The forced resonance method is reliable when applied within the confines of the analysis assumptions. It is meant to augment the toolbox of vibration-based Coulomb and viscous damping identification methods. The simplicity of the method is on par with common methods for estimating viscous or Coulomb parameters in linear oscillators with single-source damping, and the dual-damped free-vibration decrement method. Since the method is based on an analytical solution, it can also serve as a benchmark in the continuing development of damping identification schemes for more general systems, for which analytical solutions may not be available.

7 ACKNOWLEDGEMENT

This work was supported by the National Science Council (NSC892212E131001) of the Republic of China, Taiwan, and the National Science Foundation (CMS-9624347) of the USA.

8 REFERENCES

[1] Den Hartog, J. P., 1931, "Forced Vibration with Combined Coulomb and Viscous Damping," *Transactions of the American Society of Mechanical Engineering*, Vol.**53**, pp.107-115.

[2] Hundal, M. S., 1979, "Response of a Base Excited System with Coulomb and Viscous Friction," *Journal of Sound and Vibration*, Vol.**64**, pp.371-378.

[3] Jacobsen, L. S. and Ayre, R. S., 1958, *Engineering Vibrations*, McGraw-Hill, New York.

[4] Helmholtz, H. L. F., 1877, *On the Sensations of Tone as Physiological Basis for the Theory of Music*, translation by A. J. Ellis of Die Lehre von den Tonempfindungen, forth edition; first edition published in 1863, New York: Dover, pp.406.

[5] Rayleigh, Lord, 1877, *The Theory of Sound,* Vol. 1, reprinted by Dover, New York, 1945, pp.46-51.

[6] H. Lorenz, 1924, *Lehrbuch der Technischen Physik. Erster Band: Technische Mechanik Starrer Gebilde*. Berlin: Verlag von Julius Springer.

[7] Watari, A., 1969, *Kikai-rikigaku*, Kyouritsu (publisher).

[8] Liang, J.-W. and Feeny, B. F., 1998, "Identifying Coulomb and Viscous Friction from Free-Vibration Decrements," *Nonlinear Dynamics*, Vol.**16**, pp.337-347.

[9] Feeny, B. F. and Liang, J.-W., 1996, "A Decrement Method for the Simultaneous Estimation of Coulomb and Viscous Friction," *Journal of Sound and Vibration*, Vol.**195**, No.1, pp.149-154.

[10] Tomlinson, G. R. and Hibbert, J. H., 1979, "Identification of the Dynamic Characteristics of a Structure with Coulomb Friction," *Journal of Sound and Vibration*, **64**(2), pp. 233-242.

[11] Tomlinson, G. R., 1980, "An Analysis of the Distortion Effects of Coulomb Damping on the Vector Plots of Lightly Damped System," *Journal of Sound and Vibration*, **71**(3), pp.443-451.

[12] Stanway, R., Sproston, J. L., and Stevens, N. G., 1985, "A Note on Parameter Estimation in Nonlinear Vibrating Systems," *Proc. Instn Mech. Engrs,* Vol. **199**, no. C1, pp.79-84.

[13] Yao, GZ, Meng G., and Fang, T., 1997, "Parameter Estimation and Damping Performance of Electro-Rheological Dampers," *Journal of Sound and Vibration*, Vol. **204(4)**, pp. 575-584.

[14]

[16] Shaw, S. W., 1986, "On the Dynamic Response of a System with Dry Friction," *Journal of Sound and Vibration*, Vol.**108**, No.2, pp.305-325.
[17] Marui, E. and Kato, S., 1984, "Forced Vibration of a Base-Excited Single-Degree-of-Freedom System with Coulomb Friction," *Transactions of ASME, Journal of Dynamical Systems, Measurement, and Control*, Vol.**106**, pp.280-285.
[18] THK, 1996, "Linear Motion System," THK Co., Ltd., Catalog No.200-1AE, Tokyo, Japan.
[19] Yeaple F., 1986, "Precision Linear Bearings Speed Up Chip Handler," *Design News*, Vol.42, No.**18**, pp.86-87. USA.
[20] Culley S. J., van Raalte N. J., 1991, "The Modeling of Linear Motion Systems at the Design Concept Stage," *Journal of Engineering Design*, Vol.**2**, No.4, pp.303-19. UK.
[21] Anon, 1994, "Linear Motion Systems," *Industrial Lubrication and Tribology*, Vol.**46**, No.6, pp.12-21.
[22] Liang, J.-W. and Feeny, B. F., 1998, "A Comparison between Direct and Indirect Friction Measurements in a Forced Oscillator," *Journal of Applied Mechanics*, Vol.**65**, No.3, pp.783-786.
[23] Antoniou, S. S., Cameron, A., and Gentle, C. R., 1976, "The Friction-Speed Relation from Stick-Slip Data," *Wear*, **36**:235-254.
[24] Liang, J.-W., 1996, "Characterizing the Low-Order Friction Dynamics in a Forced Oscillator," Ph.D. Thesis, Michigan State University, East Lansing, MI.
[25] Liang, J.-W. and Feeny, B. F., 1998, "Dynamical Friction Behavior in a Forced Oscillator with a Compliant Contact," *Journal of Applied Mechanics*, Vol.**65**, No.1, pp.250-257.
[26] Hinrichs, N., Osetreich, M., and Popp, K., 1998, "On the Modeling of Friction Oscillator," *Journal of Sound and Vibration*, Vol.**216**, No.3, pp.435-459.
[27] Harnoy, A., Friedland, B. and Rachor, H., 1994, "Modeling and Simulation of Elastic and Friction Force in Lubricated Bearing for Precise Motion Control," *Wear*, Vol.**172**, pp.155-165.
[28] McMillan, A. J., 1997, "A Non-Linear Friction Model for Self-Excited Vibration," *Journal of Sound and Vibration*, Vol.**205**, No.3, pp.323-335.
[29] Kappagantu, R. V. and Feeny, B. F., 2000, "Part 1: Dynamical Characterization of a Frictionally Excited Beam," *Nonlinear Dynamics*, Vol.**22**, No.4, pp.317-333.
[30] Kappagantu, R. V. and Feeny, B. F., 2000, "Part 2: Proper Orthogonal Modal Modeling of a Frictionally Excited Beam," *Nonlinear Dynamics*, Vol.**23**, No.1, pp.1-11.
[31] Ibrahim, R. A., 1994, "Friction-Induced Vibration, Chatter, Squeal and Chaos," *ASME Applied Mechanics Reviews*, Vol.**47**, No.7, pp.209-253.
[32] Griffin, J. H., 1980, "Friction Damping of Resonant Stresses in Gas Turbine Engine Airfoils," *Journal of Engineering for Power*, Vol.**102**, pp.329-333.
[33] Wang, J.-H., 1996, "Design of a Friction Damper to Control Vibration of Turbine Blades," *Dynamics with Friction: Modeling, Analysis, and Experiments*, A. Guran, F. Pfeiffer and K. Popp eds., World Scientific, Singapore, pp.169-195.
[34] Wang, Y., 1996, "An Analytical Solution for Periodic Response of Elastic-Friction Damped Systems," *Journal of Sound and Vibration*, Vol.**189**, No.3, pp.299-313.
[35] Guillen, J. and Pierre, C., 1996, "Analysis of the Forced Response of Dry-Friction Damped Structural Systems Using an Efficient Hybrid Frequency-Time Method," *Nonlinear Dynamics and Controls*, ASME DE-Vol.**91**, pp.41-50.
[36] Sanliturk, K. Y. and Ewins, D. J., 1996, "Modeling Two-Dimensional Friction Contact and its Application Using Harmonic Balance Method," *Journal of Sound and Vibration,* Vol.**193**, No.2, pp.511-524.
[37] Ferri, A. A. and Heck, B. S., 1998 "Vibration Analysis of Dry Friction Damped Turbine Blades Using Singular Perturbation Theory," *Journal of Vibration and Acoustics*, Vol.120, No.**2**, pp.588-595.
[38] Hess, D. P. and Soom, A., 1990, "Friction at a Lubricated Line Contact Operating at

Oscillating Sliding Velocities," *Journal of Tribology*, **112**:147-152.
[39] Rice, J. R. and Ruina, A. L., 1983, "Stability of Steady Friction Slipping," *Journal of Applied Mechanics*, **50**:343-349.
[40] Dieterich, J. H., 1991, "Micro-mechanics of Slip Instabilities with Rate- and State-Dependent Friction," volume Fall Meeting Abstract, Volume **324**, Eos, Trans., Am. Geophys. Union.
[41] Ruina, A., 1980, Friction Laws and Instabilities: A Quasistatic Analysis of Some Dry Frictional Behavior, *PhD Thesis*, Division of Engineering, Brown University.
[42] Canudas de Wit, C., Olsson, H., Astrom, K. J., Lischinsky, P., 1995, "A New Model fro Control of Systems with Friction," *IEEE Transactions on Automatic Control* **40**(3): 419-425.
[43] Haessig, D. A. and Friedland, B. 1991, "On the modeling and simulation of friction," *Journal of Dynamic Systems, Measurement and Control,* Vol. **113**, 354-362.
[44] Oden, J. T. and Martins, J. A. C., 1985, "Models and Computational Methods for Dynamic Friction Phenomena," *Comput. Mech. Appl. Mech. Eng.*, **52(1-3)** pp.527-634.
[45] Tolstoi, D. M., 1967, "Significance of the Normal Degree of Freedom and Natural Normal Vibrations in Contact Friction," *Wear*, **10**:199-213.
[46] Dankowicz, H., 1999, "On the Modeling of Dynamic Friction Phenomena," *Zeitschrift fuer angewandte Mathematik und Mechanik* **79**(6) 399-409.
[A] Iourtchenko, D. V. and Dimentberg, M. F., 2002, "In-service identification of nonlinear damping from measrued random vibration," *Journal of Sound and Vibration* **255**(3) 549-554.
[B] Dimentberg, M. F., 1968, "Determination of Nonlinear Damping Function From Forced Vibration Test of a SDOF System," *Mechanica Tverdogo Tela*, N.2, 32-34 (in Russian).
[C] Iourtchenko, D. V., Duval, L., and Dimentberg, M. F., 2002, "The Damping Identification for Certain SDOF Systems," *Proceedings of the SECTAM-XX, Developments in Theoretical and Applied Mechanics,* April 16-18, Callaway Gardens, Pine Mountain, GA, 535-538.
[D] Chen, Q. and Tomlinson, G. R., 1996, "Parametric Identificaction of Systems with Dry Friction and Nonlinear Stiffness Using a Time Series Model," *Journal of Vibration and Acoustics* **118** 252-263.

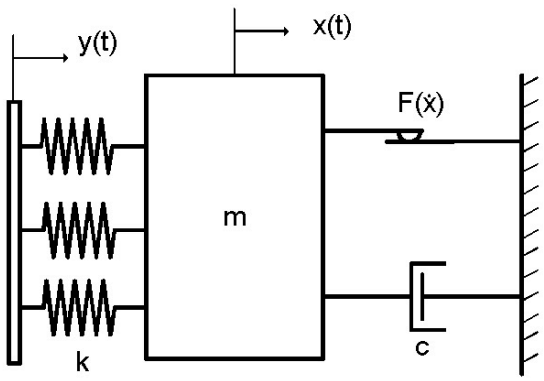

Figure 1: A schematic diagram depicting a single-degree-of-freedom oscillator with viscous, Coulomb friction and base excitation.

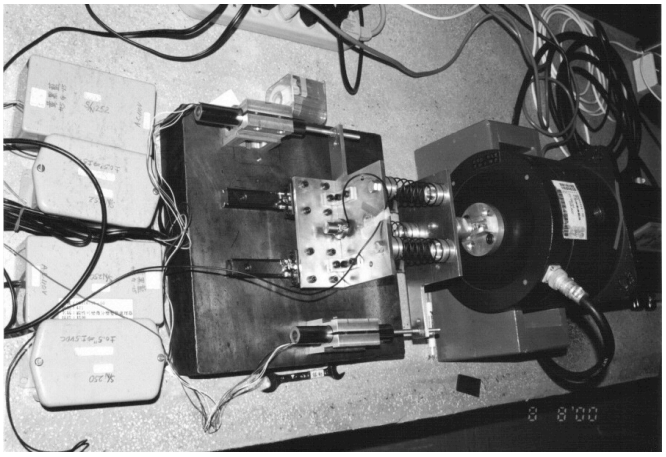

Figure 2: A photograph of experimental set-up illustrating the linear-bearing systems, the electromagnetic shaker, the LVDTs, etc.

Table 1: The input/output amplitudes of a numerical example

Y_i	x_i
$Y_1 = 0.10$	$x_1 = 0.186078$
$Y_2 = 0.20$	$x_2 = 0.436118$
$Y_3 = 0.50$	$x_3 = 1.186141$
$Y_4 = 0.60$	$x_4 = 1.436144$

Table 2: Numerical simulation results showing high accuracies in estimations using the forced-resonance method and amplitude pairs ((Y_1, x_1) , (Y_4, x_4)) of Table 1.

ζ	$\widetilde{\xi}$	e_ζ
0.2	0.199989	0.0055%
c	$\widetilde{c}$	e_c
4.0	3.99978	0.0055%
F_o	$\widetilde{F}_o$	e_{F_o}
2.0	2.0028	0.14%

Table 3: The damping estimations of the linear-bearing systems obtained from the free-vibration decrement method. The left-most estimates are for the higher amplitude segment of the free response, and the right-most estimates are for the lower amplitude segment.

No.	$\tilde{\xi}$	$\tilde{x}_f$ (mm)	$\tilde{\xi}$	$\tilde{x}_f$ (mm)
1	0.0990	0.566	0.0634	0.965
2	0.0962	0.581	0.0607	1.010
3	0.0911	0.683	0.0712	0.887
4	0.0884	0.719	0.0678	0.949
5	0.0944	0.639	0.0666	0.948
6	0.0793	0.863	0.0828	0.828
7	0.0804	0.839	0.0739	0.906
8	0.0849	0.791	0.0741	0.898
9	0.0850	0.789	0.0788	0.847
10	0.0813	0.851	0.0842	0.825
11	0.1045	0.532	0.0639	0.992
12	0.0841	0.808	0.0753	0.899
13	0.0836	0.832	0.0854	0.817
14	0.0969	0.649	0.0713	0.909
15	0.1078	0.513	0.0674	0.951
16	0.0924	0.707	0.0729	0.904
17	0.0963	0.703	0.0802	0.850

Table 4: Experimental estimations of damping parameters of the linear-bearing system.

Method	$\tilde{\xi}_i$	$\tilde{F}_{oi}$ (N)
Resonance method (least-squares fit with the whole data)	$\tilde{\xi}_1 = 0.0987$	$\tilde{F}_{o1} = 4.39$
Resonance method (least-squares fit with the lower 3/5 of the data)	$\tilde{\xi}_{3/5} = 0.126$	$\tilde{F}_{o_{3/5}} = 3.91$
Resonance method (least-squares fit with the lower 2/5 of the data)	$\tilde{\xi}_{2/5} = 0.142$	$\tilde{F}_{o_{2/5}} = 3.69$
Free-vibration decrement method	$\tilde{\xi}_{2eq} = 0.137$	$\tilde{F}_{o2eq} = 3.52$

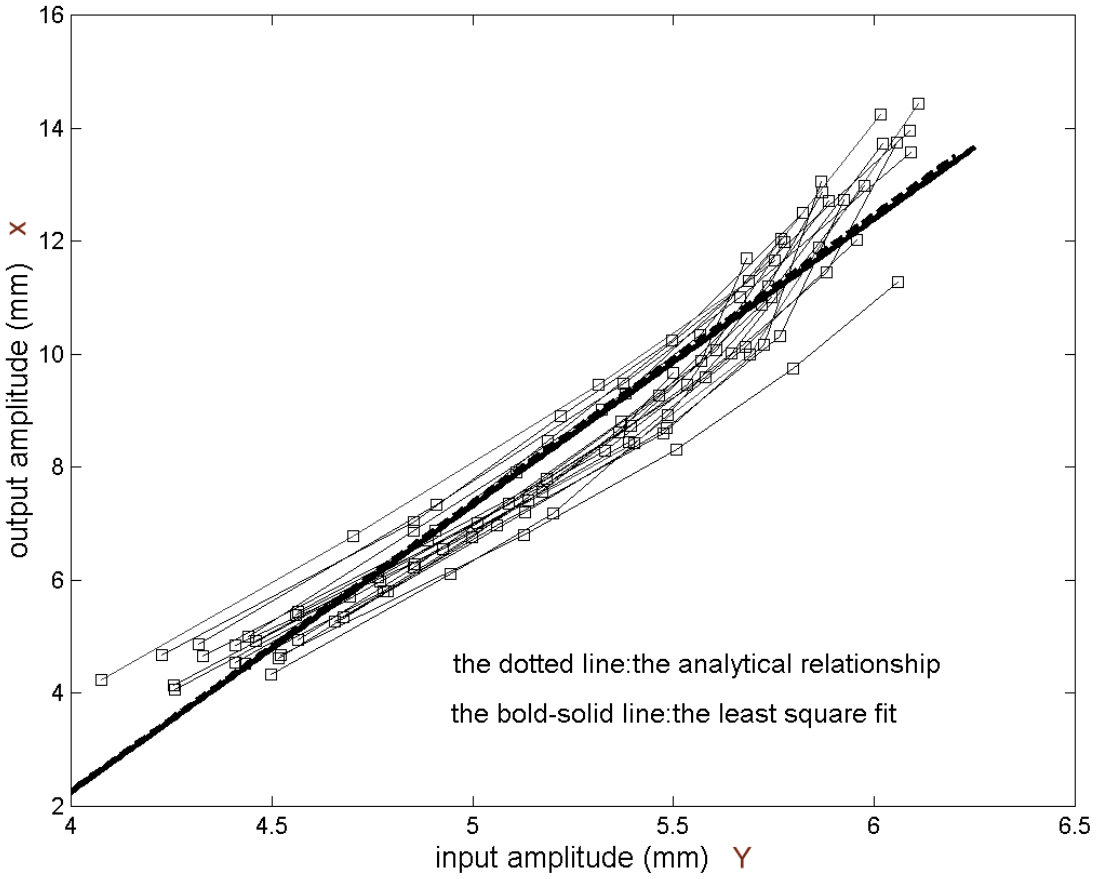

Figure 3: The experimental input-output amplitude relationships and the least-squares damping estimation.

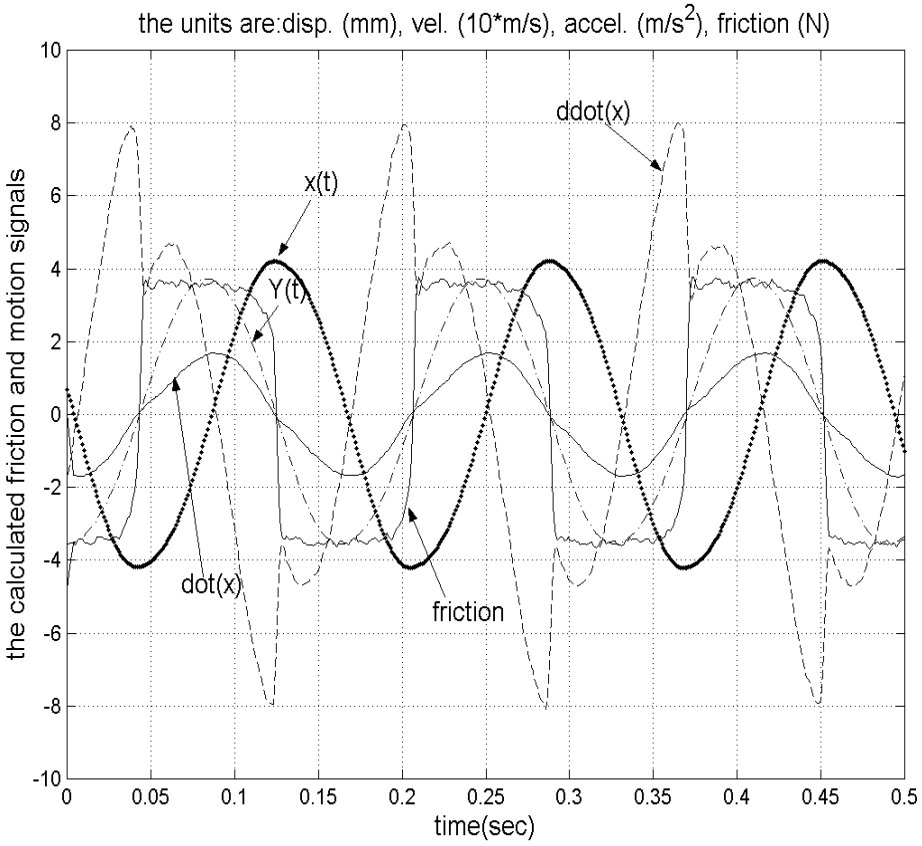

Figure 4: A typical time history depicting responses of input, output, and the calculated friction force for a sliding case.

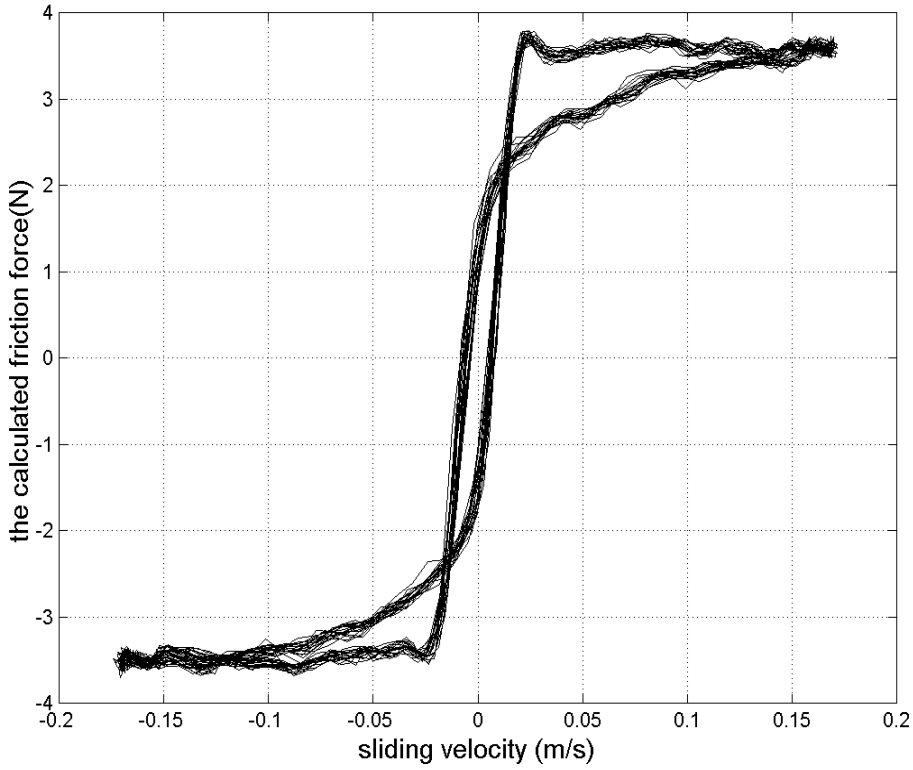

Figure 5: The friction-velocity plot showing abundant dynamics including contact

compliance, memory effect, stochastic sliding, etc., for a sliding motion case.

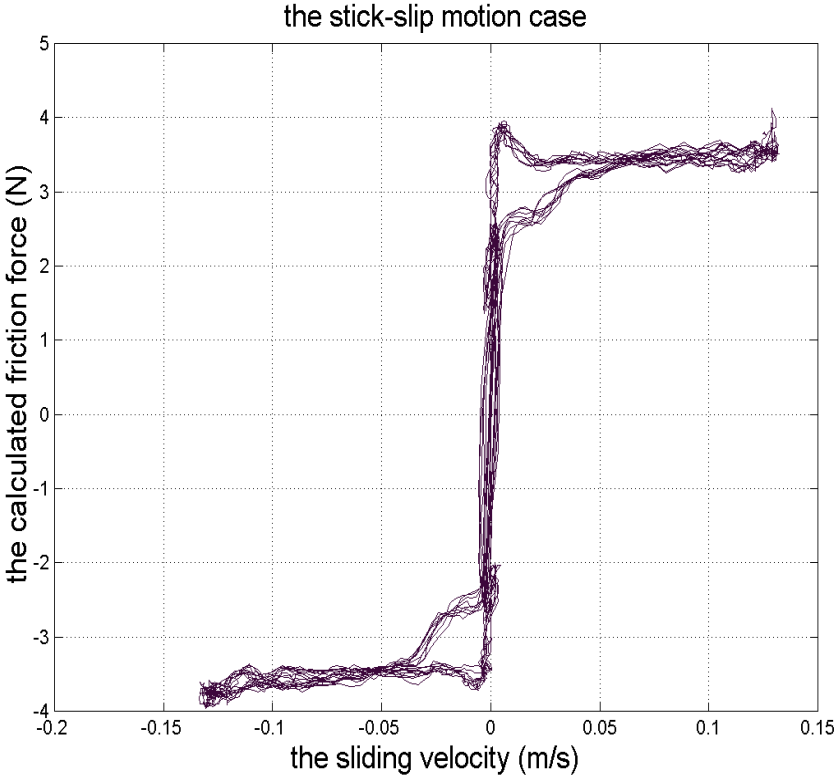

Figure 6: The friction-velocity plot for a stick-slip response.